THE JOURNAL OF BIOLOGICAL CHEMISTRY
Vol. 277, No. 7, Issue of February 15, pp. 5308–5314, 2002
Printed in U.S.A.

Translocation Activity of C-terminal Domain of Pestivirus E^{rns} and Ribotoxin L3 Loop*

Received for publication, May 8, 2001, and in revised form, October 16, 2001
Published, JBC Papers in Press, October 22, 2001, DOI 10.1074/jbc.M104147200

Johannes P. M. Langedijk‡

From the Department of Mammalian Virology, Institute for Animal Science and Health (ID-Lelystad), P.O. Box 65, 8200 AB, Lelystad, The Netherlands and Pepscan Systems, Inc., P.O. Box 2098, 8203 AB Lelystad, The Netherlands

The pestivirus envelope glycoprotein E^{rns} has RNase activity and therefore was suspected to enter cells to cleave RNA. The protein contains an RNase domain with a C-terminal extension, which shows homology with a membrane-active peptide. The modular architecture and the C-terminal homology suggested that the C terminus could be responsible for the presumed translocation. Peptides corresponding to the C-terminal domain of E^{rns} and also the homologous L3 loop of ribotoxin II were indeed able to translocate across the eukaryotic cell membrane and were targeted to the nucleoli. The entire E^{rns} protein was also able to translocate into the cell. Furthermore, other labeled proteins and even active enzymes could be transported inside the cell when they were attached to the C-terminal E^{rns} peptide. Translocation was energy-independent and not mediated by a protein receptor. The peptides showed no specificity for cell type or species.

Classical swine fever virus (CSFV),[1] bovine viral diarrhea virus (BVDV), and border disease virus (BDV) belong to the genus *Pestivirus* of the Flaviviridae family (1). CSFV is restricted to swine, whereas BVDV and BDV have been isolated from several species such as cattle, swine, sheep, deer, and giraffes (2). The disease is characterized by fever and hemorrhages and can run an acute or chronic course. Pestiviruses are plus-stranded RNA viruses whose genome comprises one long open reading frame (3–5). The structural proteins include a nucleocapsid protein C and three envelope glycoproteins E^{rns}, E1 and E2 (6).

The envelope glycoprotein E^{rns} is a disulfide-linked homodimer of ~90 kDa, and approximately half of the molecular weight is contributed by carbohydrates (7, 8). It is found on the surface of pestivirus-infected cells and is secreted in the medium (8). E^{rns} was able to bind many cell types (9), and binding of E^{rns} is probably mediated by glycosaminoglycans (10, 11). Two stretches of E^{rns} show sequence homology with ribonuclease Rh, a new class of microbial ribonuclease of *Rhizopus niveus*, member of the T_2/S RNase superfamily (12). In line with this homology, E^{rns} indeed contains RNase activity (13, 14). E^{rns} shows immunosuppressive activity since it induced apoptosis in ConA-stimulated T-cells of several species (15). However, the function for its RNase activity remains elusive. Because an extracellular, secreted protein with RNase activity most likely has an intracellular target, it was anticipated that the molecule had some kind of way to enter the cell.

This study describes a modular architecture of the E^{rns} protein and shows that the C-terminal domain was able to translocate across eukaryotic cell membranes. It was verified that also the full-length E^{rns} was translocated into cells and the C-terminal E^{rns} domain could be used as a general transport peptide to bring large enzymes into the cell. The basic E^{rns} peptide seems to have a similar ability to translocate proteins as do recently developed carrier peptides like HIV-1 Tat-(48–60) and Antennapedia-(43–58) (16–18).

EXPERIMENTAL PROCEDURES

Peptide Synthesis—Peptides were selected from the C-terminal region (residues 191–227) of CSFV E^{rns}, strain Alfort 187 (19), the L3 loop of restrictocin (residues 59–88) (20), and magainin-1 (21). Also an unrelated control peptide was synthesized of a length comparable with the pestivirus E^{rns} peptide. CSFV: acetyl-ENARQGAARVTSWLGRQLRIAGKRLEGRSKTWFGAYA-COOH; CSFV: biotin-ENARQGAARVTSWLGRQLRIAGKRLEGRSKTWFGAYA-COOH; L3: biotin-GNGKLIKGRTPIKFGKADCDRPPKHSQNGMGK-NH_2; Mag-1: biotin-GIGKFLHSAGKFGKAFVGEIMKS-NH_2; Control: biotin-WWKGTLTFTAKMRSSNMWNPEQQHTTTAENIGKYIPNIGG-NH_2. Also panels of truncated CSFV E^{rns} peptides and restrictocin L3 peptides were synthesized to elucidate the minimal membrane active region (see Tables I and II).

Peptides were synthesized according to standard procedures on an Applied Biosystems 430A synthesizer or on a Hamilton Microlab 2200 (Reno, NV) using Fmoc/HBTU (2"-(1H-benzotriazole-1-yl)-1,1,3,3-tetramethyluronium hexafluorophosphate) chemistry. (22) After removal of the last Fmoc group, peptides were biotinylated using 0.45 M biotin, which was activated for 15 min in 0.45 M HBTU/1-hydroxybenzotriazole in *N*,*N*-dimethylformamide. After 1 h the reaction was stopped by washing five times with *N*-methyl-2-pyrrolidone and three times with EtOH. The purity of the peptides was >90% as determined by analytical liquid chromatography/mass spectrometry.

Recombinant Protein and Translocation Assay—E^{rns} of CSFV strain C (amino acids 268–494 of the CSFV polyprotein) was expressed by a recombinant baculovirus in sf21 cells as described previously (10, 14). Translocation of the peptide across the plasma membrane was studied by incubation of live cells in suspension or subconfluent monolayers on coverslips with biotinylated peptide (200–0.4 μg/ml culture medium) for 1, 10, 30, 45, or 120 min. After the time period, cells were fixed with 4% paraformaldehyde or cold methanol and labeled with streptavidin-FITC as described above. Fixed cells were inspected with fluorescence microscopy. Internalization was established with confocal microscopy. Comparison of translocation activity of different peptides was done by visual inspection of fluorescence intensity of titrated peptides that were stained by streptavidin-FITC. The following cell lines were used: A72, canine fibroblast tumor cells; MDCK, canine kidney epithelial cells; CCO, sheat-fish ovary cells; EK-1, Eel kidney cells; CHS-E, salmon embryonal cells; BUEC, bovine umbilical endothelial cells; BFDL, bovine fetal diploïd lung cells (fibroblast); PUEC, porcine umbilical endothelial cells; HT 29, colorectal adenocarcinoma, colon epithelial cells; CaCo-2, colorectal adenocarcinoma, colon epithelial cells; HeLa, adenocarcinoma, cervix; Vero, normal monkey kidney epithelial cells; SK6,

* The costs of publication of this article were defrayed in part by the payment of page charges. This article must therefore be hereby marked "*advertisement*" in accordance with 18 U.S.C. Section 1734 solely to indicate this fact.

‡ To whom correspondence should be addressed: Dept. of Mammalian Virology, Inst. for Animal Science and Health (ID-Lelystad), Edelhertweg 15, P.O. Box 65, 8200 AB, Lelystad, The Netherlands. Tel.: 31-320-238271; Fax: 31-320-238120; Email: j.p.m.langedijk@id.wag-ur.nl.

[1] The abbreviations used are: CSFV, classical swine fever virus; Fmoc, *N*-(9-fluorenyl)methoxycarbonyl; FITC, fluorescein isothiocyanate; HRP, horseradish peroxidase.

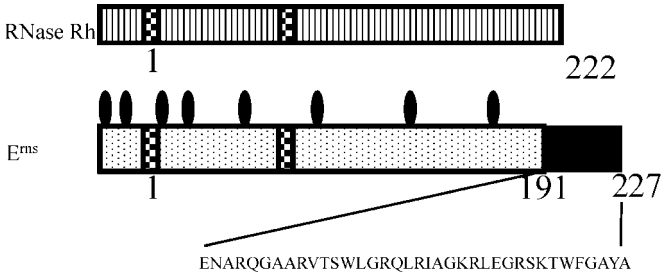

FIG. 1. **Schematic representation of alignment of pestivirus E^{rns} with RNase Rh that indicates the modular organization of E^{rns}.** E^{rns} consists of an RNase domain (*dotted*) and a C-terminal membrane active domain (*filled black*). Strongly homologous RNase active site domains are shown as *checkered boxes*. Potential glycosylation sites are shown as *ellipses*.

swine kidney cells; NPTh, newborn pig thyroid cells; ECTC, embryonal calf thyroid cells; MDBK, normal bovine kidney epithelial cells; EBTr, epithelial bovine trachea cells; bovine sperm cells; Sp20, mouse myeloma B-cells.

Enzymatic Staining and Confocal Cell Microscopy—Enzymatic activity of translocated streptavidin-horseradish peroxidase (DAKO) was assessed by staining with 0.02% 3-amino-9-ethylcarbazole for 5 min, and translocated streptavidin-β-galactosidase (Sigma) was assessed by staining with 0.1% 5-bromo-4-chloro-3-indolyl β-D-galactopyranoside (X-gal) for 20 min. Stained cells as described above were analyzed using a confocal laser scanning microscope with an Argon laser using an excitation wavelength of 488 nm and an emission of 515 nm using a blue high sensitive block.

Hemolytic Assay—Hemolytic activity of various peptide concentrations were determined by incubation with human, guinea pig, or sheep erythrocyte suspensions (final erythrocyte concentration, 1% v/v) for 1 h at 37 °C. After cooling and centrifugation, the optical density of the supernatants were measured at 540 nm. Peptide concentrations causing 50% hemolysis (EC_{50}) were derived from the dose-response curves.

Generation of Transmembrane Potential—Erythrocytes were suspended in a buffer (10 mM Hepes/150 mM (NaCl + KCl)/1 mM EDTA, pH 7.4) containing 97 mM (−9 mV) or 4 mM (−70 mV) K^+. The resting potential of −9 mV approximates the resting potential of human erythrocytes (23). The transmembrane potential was generated by addition of valinomycin (6.7 μM for 1% hematocrit).

Clonogenicity of Mammalian Cells—HeLa or EBTr cells were cultured in Dulbecco's modified Eagle's medium, supplemented with 20% fetal bovine serum and antibiotics in a humidified atmosphere supplied with 5% CO_2 at 37 °C. Exponentially growing cells were treated with trypsin and transferred to wells of a 96-well microtiter plate. Resulting in ~300 cells for each 30 μl of growth medium containing various concentrations of peptide. After incubation for 75 min (the plates were incubated upside down to avoid anchorage) the cells were transferred and plated in wells of tissue culture plates that contained 100 μl of growth medium. Cell growth was checked after 3–6 days.

Colocalization Stains—Nucleoli-specific staining was performed as described (24). In short, cells were incubated for 30 min with biotinylated peptide as described above. After washing, the cells were fixed with methanol at −20 °C, washed with sodium acetate buffer (0.01 M, pH 4.9). Cells were washed and incubated with 40 μl of streptavidin-Texas Red (10 μg/ml) at 37 °C, incubated with Acridine Orange (1 μg/ml; room temperature, pH 4.9), washed, and incubated with 0.01% methyl green (pH 4.9). Cells were inspected with fluorescence microscopy at 490, 595/615, and 503/515 nm.

RESULTS

Sequence Analysis—A structural model of E^{rns} was built by homology modeling based on an approximate sequence alignment of pestivirus E^{rns} with ribonuclease Rh (RNase Rh).[2] The alignment, which is shown schematically in Fig. 1, showed that the 37 C-terminal residues of E^{rns} do not align with RNase Rh and seem to form a separate region. The C-terminal region has no potential glycosylation sites, has a high number of positive charges and a high score for amphipathic helicity. A helical

[2] J. P. M. Langedijk, P. van Veelen, W. M. Schaaper, R. H. Meloen, M. M. Hulst, manuscript in preparation.

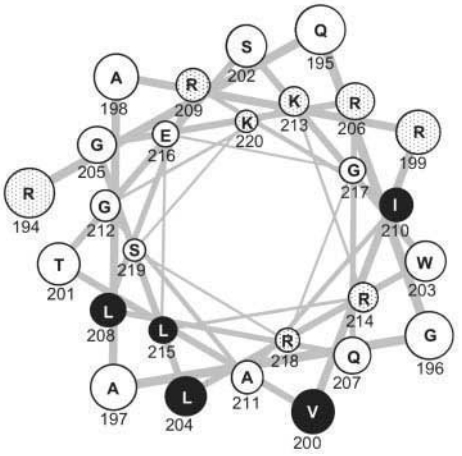

FIG. 2. **Helical wheel representation of residues 194–220 of CSFV E^{rns}.** Hydrophobic residues (*filled black*) and positive residues (*dotted)* are indicated.

wheel representation of residues 194–220 shows an amphipathic helix with a hydrophobic face and a positively charged face (Fig. 2). The only three residues that do not correspond with the amphipathicity are Ile-210, Arg-214, and Arg-218. Such a positively charged domain in an RNase molecule is not unique for E^{rns} but has also been observed in type II ribotoxins, another class of RNases. This class of RNases are extracellular cytotoxins that are able to translocate across phospholipid bilayers (25) and hydrolyze the large ribosomal RNA (26). Although ribotoxins are known to enter cells, it is not known which region of the protein is responsible for translocation. The type II ribotoxins like α-sarcin and restrictocin contain a large inserted L3 loop (residue 53–91) compared with other RNases of the T1 superfamily (27, 28). This loop has structural similarity (but no sequence similarity) to loops found in lectin sugar-binding domains and may be responsible for the ribotoxins ability to bind the cell surface (27). The C-terminal domain of E^{rns} has approximately the same length and contains similar sequence motifs as the ribotoxin II L3 loop (Fig. 3). Although the sequence similarity between the ribotoxin L3 loop and the C terminus of E^{rns} is low (Fig. 3), it is higher than the sequence similarity between L3 and the structurally similar lectin binding domains (27). Although the ribotoxin L3 loop is also positively charged, it has no apparent amphipathic character. Another interesting homology of the E^{rns} C-terminal region is with the membrane-interacting peptide magainin. The center of the E^{rns} peptide has sequence homology with the N-terminal half of magainin (Fig. 3). This homology is even higher compared with the homology of magainin with other pore-forming peptides that have been described (29).

E^{rns} Translocation—To test whether the entire E^{rns} dimer was able to translocate into epithelial cells, recombinant E^{rns} of C-strain virus was incubated for 45 min with EBTr cells grown on coverslips overnight. After washing with phosphate-buffered saline the cells were fixed with cold methanol, and E^{rns} was detected by incubation with a mix of monoclonal antibodies 140.1 and C5 (1/200) directed against E^{rns} and a second incubation with rabbit anti mouse-FITC (1/70) (F0261, DAKO). E^{rns} could be detected outside as well as inside the cell by confocal microscopy. Accumulation could be observed around the nucleus (Fig. 4).

Peptide Translocation—Because the C-terminal region was identified as a separate domain that shows homology with a pore-forming peptide and a peptide that probably interacts with cell surfaces, peptides were synthesized corresponding to the C-terminal domain and tested for translocation activity.

```
E N A R Q G A A R V T S W L G R Q L R I A G K R L E G R - S K T W F G A Y A   CSFV
E G A R Q G A A R V T S W L G R Q L S T A G K R L E G R - S K T W F G A Y A   CSFVb
E S A R Q G T A K L T T W L G R Q L K K L G K K L E N K - S K T W F G A Y A   BVDV
E G A R K G A A K L T T W L G K Q L R I L G K K L E S K - S K T W F G A H A   bvdv-2
E N A R Q G A A K L T S W L G K Q L G I M G K K L E H K - S K T W F G A N A   BDV
                  G I G K F L H S A G K F - - G K - - - A F V G E I M K S   Magainin
- - - - - - D G N G K L I K G R T P I K F G K A D C D R P P K H S Q N G M G K   Restrictocin
```

FIG. 3. **Sequence alignment of pestivirus E^{rns} C-terminal domains with magainin-1 and the L3 loop of restrictocin-(21,28).** Residues within one distance unit from CSFV are *boxed*. Gaps are indicated by *dashes*.

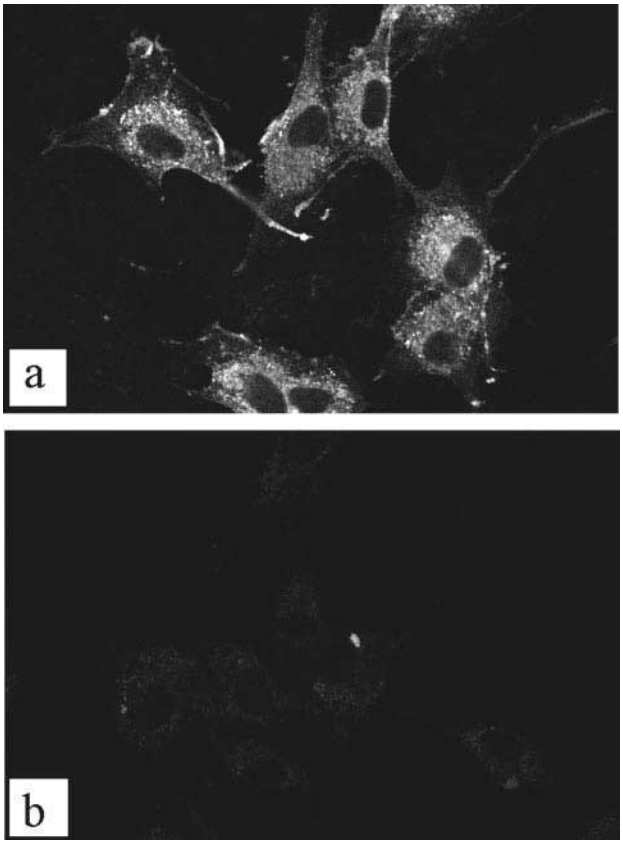

FIG. 4. **Distribution of purified recombinant CSFV E^{rns} strain C (*a*) or supernatant of mock-infected sf21 cells (*b*).** EBTr cells were incubated with 1 μM E^{rns} for 45 min. Fixed cells were incubated with a mix of monoclonals directed against E^{rns}, and subsequently incubated with rabbit anti mouse-FITC. Fluorescent micrographs using confocal microscopy (600 X).

Cell suspensions (mouse myeloma and bovine sperm) and subconfluent monolayers of 17 different cell types (see "Experimental Procedures") were incubated for 1 h with biotinylated E^{rns} peptide and fixed with cold methanol. Inspection with fluorescent microscopy and confocal microscopy showed that the peptide had penetrated inside all tested cell types. No obvious differences in cellular distribution or intensity were observed between cell types. Next, EBTr cells were incubated with biotinylated E^{rns} peptide and fixed after different time intervals. The peptide entered the cell within 1 min and optimal fluorescence was established after 30 min (Fig. 5). After longer incubation times (3 h) the image was less clear. It is not known whether this is due to cellular changes or proteolysis of the peptide. The translocated peptide was distributed around the nucleus in membranous parts in the cytosol and, in contrast to the native protein, clear accumulation in the nucleoli was observed. The peptide has a similar intracellular localization as a known transport peptide like the Antennapedia-(43–58) peptide.

Translocation was also observed at 4 °C and could not be competed by a 10-times excess of unbiotinylated E^{rns} peptide (data not shown). Therefore, the mechanism is energy-independent and not receptor mediated.

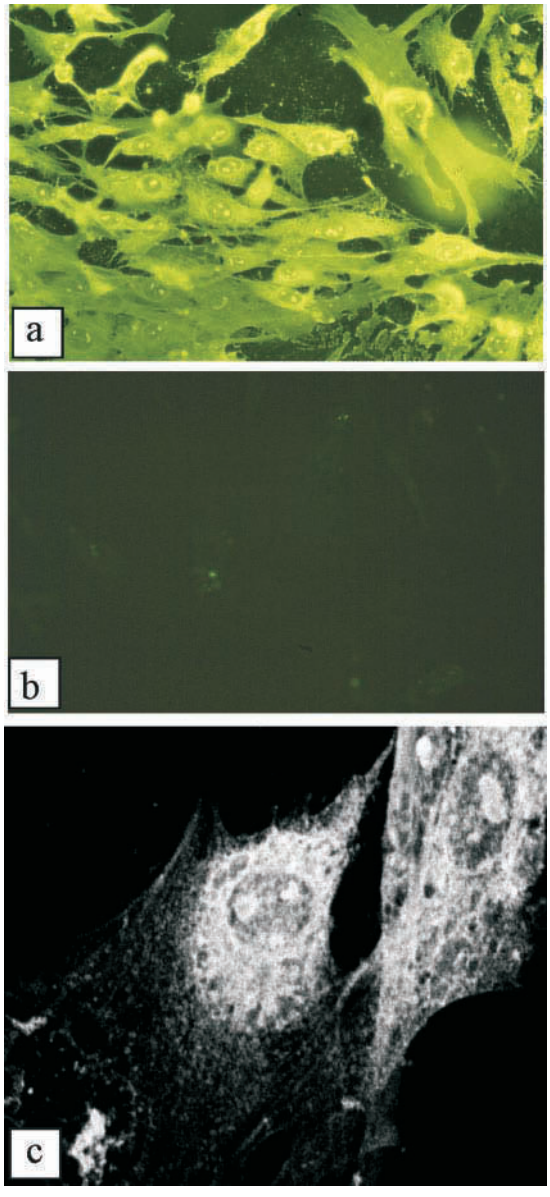

FIG. 5. **Distribution of biotinylated CSFV E^{rns} peptide (*a*, *c*) and biotinylated control peptide (*b*) (25 μM) after 30 min of incubation with subconfluent EBTr cells grown on a 10-well microscope slide.** Cells were fixed with cold methanol, and biotinylated peptide was visualized by staining with avidin-FITC for 30 min. Fluorescent micrograph (250X)(*a*, *b*) or fluorescent micrograph using confocal microscope (600X) (*c*).

Translocation of Homologous Peptides and Mapping of Translocation Region—The part of the E^{rns} C-terminal region responsible for translocation was mapped precisely by testing the translocation activity of a panel of truncations of the E^{rns} peptide and some peptides with N-terminal additions and deletions and C-terminal deletions (Table I). Deletion of the seven-most C-terminal residues and the three N-terminal residues increased the translocation activity of the peptide (Table I). The

TABLE I
Transporter peptides: Determination of minimal translocating sequence of E^{rns}

ND = not determined.

Residue number	Sequence[a]	Internalized fluorescence	Hemolysis
			mg/ml
191–227	$ENARQGAARVTSWLGRQLRIAGKRLEGRSKTWFGAYA#	++++	0.07
184–223	$DGMTNTIENARQGAARVTSWLGRQLRIAGKRLEGRSKTWF#	++++	0.15
181–220	$YLLDGMTNTIENARQGAARVTSWLGRQLRIAGKRLEGRSK#	++++	0.09
177–216	$DTALYLLDGMTNTIENARQGAARVTSWLGRQLRIAGKRLE#	++	0.23
172–211	$GSLLQDTALYLLDGMTNTIENARQGAARVTSWLGRQLRIA#	+	>0.33
191–223	$ENARQGAARVTSWLGRQLRIAGKRLEGRSKTWF#	++++	0.15
191–220	$ENARQGAARVTSWLGRQLRIAGKRLEGRSK#	++++	0.31
191–216	$ENARQGAARVTSWLGRQLRIAGKRLE#	++	>0.33
191–211	$ENARQGAARVTSWLGRQLRIA#	+	>0.33
194–220[b]	$RQGAARVTSWLGRQLRIAGKRLEGRSK#	+++++	0.26
194–218	$RQGAARVTSWLGRQLRIAGKRLEGR#	++++	ND
196–220	$GAARVTSWLGRQLRIAGKRLEGRSK#	+++	0.16
199–220	$RVTSWLGRQLRIAGKRLEGRSK#	++	0.18
202–220	$SWLGRQLRIAGKRLEGRSK#	+	>0.33
205–220	$GRQLRIAGKRLEGRSK#	+	>0.33

[a] $ = biotin; # = amide.
[b] Sequence of peptide which showed highest translocation activity.

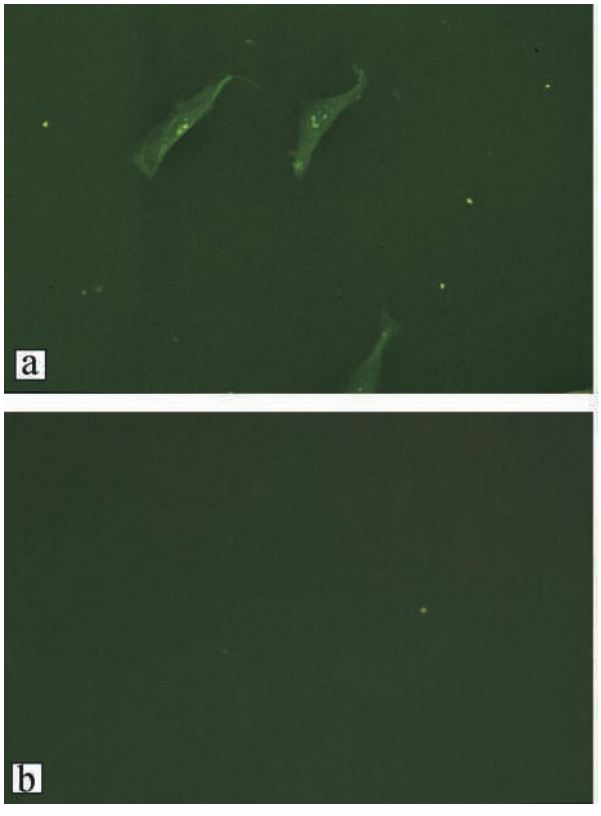

FIG. 6. **Distribution of biotinylated L3 peptide (*a*) and magainin-1 peptide (*b*) (6 μM) after 30 min of incubation with subconfluent EBTr cells grown on a 10-well microscope slide.** Cells were fixed with cold methanol, and biotinylated peptide was visualized by staining with avidin-FITC for 30 min. Fluorescent micrograph, 250X.

most active biotinylated peptide (residues 194–220) still showed fluorescence above background at 250 nM with streptavidin-FITC. Because the E^{rns} peptide showed some resemblance with the ribotoxin L3 loop and some sequence homology with magainin, these peptides were also tested for translocation activity (Fig. 6). At 54–2 μM the biotinylated E^{rns} peptide and the biotinylated L3 peptide show clear translocation activity, and the biotinylated magainin-1 peptide does not. The part of the restrictocin L3 loop responsible for translocation was mapped by testing the translocation activity of a panel of truncations of L3 loop peptides (Table II). A short 13-residue peptide N-terminal to the cysteine displayed the highest translocation activity.

TABLE II
Transporter peptides: Determination of minimal translocating sequence of restrictocin L3

Residue number	Sequence[a]	Internallized fluorescence
57–89	$GNGKLIKGRTPIKFGKADCDRPPKHSQNGMGK#	+++++
57–87	$GNGKLIKGRTPIKFGKADCDRPPKHSQNGM#	+++
60–89	$KLIKGRTPIKFGKADCDRPPKHSQNGMGK#	++++++
63–89	$KGRTPIKFGKADCDRPPKHSQNGMGK#	+++
60–73	$KLIKGRTPIKFGK#	++++++

[a] $ = biotin; # = amide.

Transport of Proteins—Next, it was tested whether the peptide could be used as a general transporter for cargoes other then E^{rns}. This was tested by coupling labeled avidin and streptavidin to the biotinylated peptide. After mixing equimolar amounts of streptavidin-FITC (60 kDa, nonglycosylated, neutral) or avidin-Texas Red (66 kDa, glycosylated, pI = 10.5) with the most active E^{rns} peptide (residues 194–220) (3 μM) it was possible to transport streptavidin-FITC and avidin-Texas Red inside the cell and the nucleus (Fig. 7). Transport seems highly efficient because internalization of the peptide-streptavidin-FITC complex was still visible at a peptide concentration 20 times lower than the uncomplexed peptide (0.05 μM compared with 1 μM). Also in the case of streptavidin transport, the amount of accumulation was the same at 37 °C and 4 °C, which suggest that also the transport of larger cargoes is independent of endocytosis. The biotinylated restrictocin L3 peptide (residues 60–89) was not able to translocate 1 μM avidin-Texas Red or streptavidin-FITC (data not shown).

Next, it was checked whether also large active enzymes could be translocated into the cell and tested for their enzymatic activity. This was tested by coupling streptavidin-horseradish peroxidase (HRP) and streptavidin-β-galactosidase to the biotinylated peptide. A preformed complex of E^{rns} peptide with streptavidin-HRP (104 kDa) and a preformed complex of E^{rns} peptide with β-galactosidase (524 kDa) was incubated with EBTr cells for 30 min. After washing, fixing with cold methanol, and incubation with the respective substrates ("Experimental Procedures"), the translocated active enzymes could be detected in the cytosol and the nucleoli (Fig. 8).

Toxicity—Effective, non-toxic transport peptides should preferably have high translocation activity and low hemolytic ac-

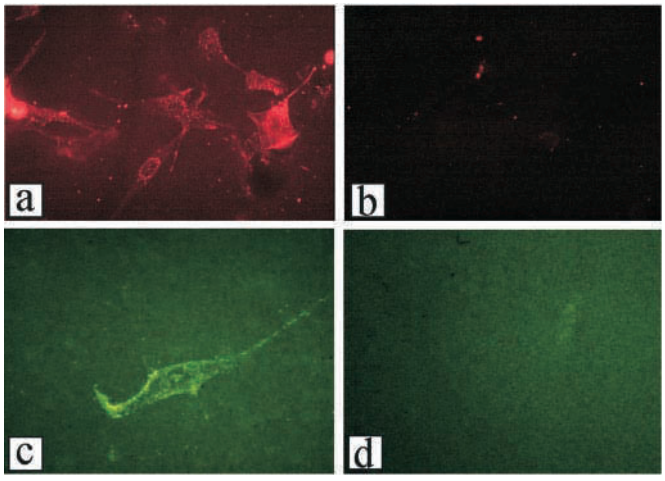

FIG. 7. **Transport of avidin and streptavidin.** EBTr cells were incubated for 30 min with a complex of biotinylated E^{rns} peptide and Avidin-Texas Red (*a*) or streptavidin-FITC (*c*) (3 μM). As a control, EBTr cells were incubated with a mixture of unbiotinylated peptide and avidin-Texas Red (*b*) or streptavidin-FITC (*d*) (3 μM). Peptide corresponds to residues 194–220 of E^{rns}.

tivity and/or toxic activity. To check whether the membrane destabilizing activity had a general toxic effect on cells, hemolytic activity, tryphan blue exclusion, and influence on cell growth was tested. EBTr cells were tested for tryphan blue leakage after peptide incubation for 30 min. Only at high concentrations of peptide (>35 μM) some tryphan blue could be determined inside the cell, especially in areas in the nucleus. Hemolysis of erythrocytes can also be indicative for lytic effect of the peptides on eukaryotic cell membranes. Hemolysis of erythrocytes from several species was tested with the panel of E^{rns} peptides (Table I). The different peptides show a broad range of hemolytic activities on guinea pig erythrocytes. The peptide with the highest translocation activity (residues 194–220) has a low hemolytic activity. No significant hemolysis was observed with sheep and human erythrocytes. The effect of the E^{rns} peptide on cell growth of HeLa cells and EBTr cells was determined in a clonogenicity assay as shown in Table III. These data correspond to the other toxicity assays and indicate that the translocation activity is much higher than the cytotoxic activity.

Membrane Potential—Because the translocation seemed energy-independent, it was tested whether the membrane potential could be the driving force for translocation. Because mem-

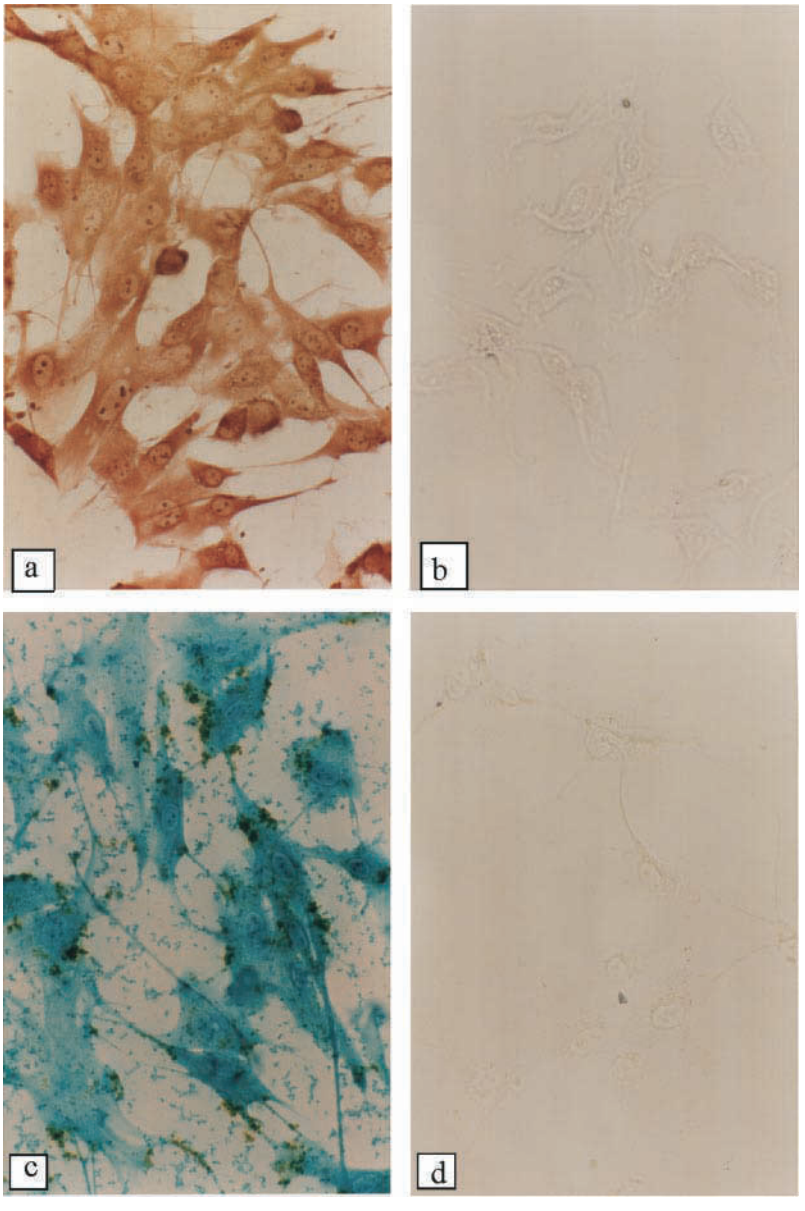

FIG. 8. **Transport of streptavidin-HRP and streptavidin-β-galactopyranoside.** EBTr cells were incubated for 30 min with a preformed complex of E^{rns} peptide with streptavidin-HRP, 0.5 μM (*a*); preformed complex of E^{rns} peptide with streptavidin-β-galactopyranoside, 2 μM (*b*); control streptavidin-HRP 0.5 μM (*c*); control streptavidin-β-galactopyranoside, 2 μM (*d*). Staining was performed as described under "Experimental Procedures."

TABLE III
Transporter peptides: Peptide concentration that inhibits cell growth

Cell type	E^{rns} peptide (191–227)	E^{rns} peptide (194–220)
	μM	μM
HeLa	50	40
EBTr	50	60

brane activity measured with a hemolysis test correlated to some extent with translocation activity, the influence of membrane potential on hemolysis of human red blood cells was tested. Hemolysis is a straightforward test to study membrane activity, and the membrane potential of erythrocytes can be easily manipulated by changing the sodium concentration in the medium. Hemolysis at membrane potentials of −9 mV and −70 mV shows that hemolysis was much higher at higher membrane potential (Fig. 9).

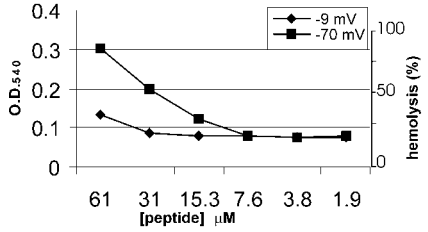

FIG. 9. **Influence of membrane potential on hemolysis of human erythrocytes.** Erythrocytes were suspended in a buffer (10 mM Hepes/150 mM (NaCl + KCl)/1 mM EDTA, pH 7.4) containing 97 mM (−9 mV) or 4 mM (−70 mV) K^+. The transmembrane potential was generated by addition of valinomycin.

DISCUSSION

The pestiviral surface protein E^{rns} is unique because it is the only known viral surface protein with RNase activity (13, 14). Although the biological function of the protein is not understood, it may be possible that, just as ribotoxins, the target for the protein is intracellular or intranuclear RNA. Therefore, we anticipated that the molecule had some kind of way to enter the cell. However, except for some specialized proteins like toxins, internalization of macromolecules can only be achieved through the classical endocytosis pathway.

In this study, it was shown that the entire recombinant E^{rns} dimer was indeed able to translocate into cells. Sequence analysis indicated that the first 190 residues of E^{rns} show homology to RNases of the T2/S superfamily and that the C-terminal 37 residues probably fold as a separate domain.[2] This C-terminal domain is non-glycosylated, highly positively charged, and amphipathic and shows a slight homology with the pore-forming, antibacterial peptide magainin, and with a large loop in type II ribotoxins, which was expected to bind cell surfaces (27). Therefore, the C-terminal domain of E^{rns} was most likely responsible for the translocation activity. It was demonstrated that indeed, a peptide of 37 residues corresponding to the C-terminal domain of E^{rns} translocates very efficiently over the plasma membrane of all tested cell types of a wide variety of species. The peptide is targeted to the nucleoli and to cytoplasmic membranes and localizes in the same areas as other known transport peptides like the HIV-1 Tat and Antennapedia peptide (data not shown).

The translocation is very fast (<1 min); it is energy-independent and receptor-independent. The independence of binding to a saturable receptor agrees with the lack of cell specificity and suggests that the peptide interacts directly with fosfolipids as has been described for another transport peptide (30). Because the hemolytic activity correlated to some extent with translocation activity, the influence was tested for membrane potential on hemolysis of human red blood cells. Fig. 9 shows that the membrane activity was dependent on the membrane potential. Since the translocation is energy-independent, the membrane potential may therefore be the driving force for translocation.

Because the elucidation of the translocating E^{rns} peptide was inspired by the homology with magainin and the ribotoxin L3 loop, it was also tested whether a peptide corresponding to the L3 loop had translocating activity. Although previously another, more hydrophobic region of α-sarcin was shown to interact with membranes (31), in this study it was shown that a more N-terminally located peptide corresponding to the restrictocin L3 loop had translocation activity (Fig. 6). Perhaps both regions contribute to membrane translocation in the native protein.

To elucidate the exact region of the peptides responsible for translocation, panels of E^{rns} peptides and restrictocin peptides with different lengths were synthesized. The most active translocating E^{rns} peptide was 10 residues shorter (residue 194–220) then the full-length C-terminal peptide of E^{rns}-(191–227), and it was less toxic (Table I). The most active translocating restrictocin L3 peptide was 13 residues long, which corresponds to the N-terminal half of the L3 loop before the cystine bridge, which divides the loop into two parts in the native protein. Just like other known transporter peptides, the mapping showed that basic residues were important for translocation activity.

The homology between the most active restrictocin L3 and the E^{rns} peptide is only two small sequence motifs (GR and GK), which is much lower compared with the homology between E^{rns} peptide and magainin, which has no translocation activity (Fig. 6). Magainin forms a perfect amphipathic helix, thus amphipathicity is not important for transport peptides. In contrast to the E^{rns} peptide, the L3 loop peptide has no amphipathicity when represented as a helix. Furthermore, the L3 loop contains a helix-breaking proline. It has been suggested that there may be several different translocation mechanisms for the different peptides and that they not necessarily have to form a helix (32). Recently, several transport peptides have been discovered that all have a very different origin, and no obvious sequence homology can be observed (16, 18, 32–34). The only resemblance is the high amount of positive charges.

The mapping experiments also proved that the peptide did not only translocate itself and a biotin molecule, but also peptide cargoes could be transported. Next, it was shown that the peptide could be used as a general transporter for proteins different from E^{rns}. Streptavidin and avidin, which have different physical characteristics, could be transported into cells when complexed to the E^{rns} peptide. The labeled proteins were targeted to the same intracellular regions as the peptide, concentrated in vesicle-like structures around the nucleus, and spread through the cytoplasm. In contrast to recombinant E^{rns}, nucleoli targeting was observed, although it was less pronounced than the peptide (Fig. 7). Even the enzymes HRP and β-galactopyranoside conjugated to streptavidin could be efficiently transported into cells when complexed with the E^{rns} peptide. Internalized enzymes retained their activity, and clear substrate conversion was observed in the nucleoli. Especially, the streptavidin-β-galactopyranoside conjugate that has a molecular mass as high as 524 kDa and a pI as low as 4.6 illustrates the remarkable efficacy of the transport peptide. In contrast, the restrictocin L3 peptide was not able to translocate the selected protein cargoes. Perhaps the difference in transport ability of the two peptides is based on the pI, which is lower for the L3 peptide (pI = 10.7) compared with the E^{rns} peptide (pI = 12.7). Accordingly, the transport ability of the peptides may increase by increasing the pI of the peptides.

Another difference between both peptides is that L3 is an internal peptide and the E^{rns} peptide is originally a terminal peptide and for that reason may be more efficient in the described experiments in which it was terminally attached.

The demonstration of a translocation domain within E^{rns} adds a novel facet to this so far poorly understood pestiviral glycoprotein and may encourage studies on how a secreted RNase is involved in the survival strategy of an RNA virus. The function of E^{rns} and the function of its RNase activity remain elusive but the translocation suggests that it may control protein synthesis and transcription in infected cells as well as non-infected cells. The E^{rns} peptide and the ribotoxin L3 peptide may be used as a delivery tool to transport a diverse set of potential therapeutics inside the cell.

Acknowledgments—I thank Rob Buijs, Mark de Groot, and Wim Schaaper for technical assistance.

REFERENCES

1. Wengler, G., Bradley, D. W., Collett, M. S., Heinz, F. X., Schlesinger, R. W., and Strauss, J. H. (1995) *Flaviviridae. Virus taxonomy. Sixth Report of the International Committee of Viruses* (Murphy, F. A., Fauquet, C. M., Bishop, D. H. L., Ghabrial, S. A., Jarvis, A. W., Martelli, G. P., Mayo, M. A., and Summers, M. D., eds) Springer Verlag, Vienna, Austria
2. Paton, D. J., Simpson, V., and Done, S. H. (1992) *Vet. Rec.* **131,** 185–188
3. Francki, R. I. B., Faquet, D. L., Knudson, D. L., Brown, F. (1991) *Arch. Virol. Suppl.* **2,** 223–233
4. Colett, M. S., Larson, R., Gold, C., Strick, D., Anderson, D. K., and Purchio, A. F. (1988) *Virology* **165,** 191–199
5. Moormann, R. J., Warmerdam, P. A., van der Meer, B., Schaaper, W. M., Wensvoort, G., and Hulst, M. M. (1990) *Virology* **177,** 184–198
6. Thiel, H. J., Stark, R., Weiland, E., Rumenapf, T., and Meyers, G. (1991) *J. Virol.* **65,** 4705–4712
7. Konig, M., Lengsfeld, T., Pauly, T., Stark, R., and Thiel, H. J. (1995) *J. Virol.* **69,** 6479–6486
8. Rumenapf, T., Unger, G., Strauss, J. H., and Thiel, H. J. (1993) *J. Virol.* **67,** 3288–3294
9. Hulst, M. M., and Moormann, R. J. (1997) *J. Gen. Virol.* **78,** 2779–2787
10. Hulst, M. M., van Gennip, H. G., and Moormann, R. J. (2000) *J. Virol.* **74,** 9553–9561
11. Iqbal, M., Flick-Smith, H., and McCauley, J. W. (2000) *J. Gen. Virol.* **81,** 451–459
12. Horiuchi, H., Yanai, K., Takagi, M., Yano, K., Wakabayashi, E., Sanda, A., Mine, S., Ohgi, K., and Irie, M. (1988) *J. Biochem. (Tokyo)* **103,** 408–418
13. Schneider, R., Unger, G., Stark, R., Schneider-Scherzer, E., and Thiel, H. J. (1993) *Science* **261,** 1169–1171
14. Hulst, M. M., Himes, G., Newbigin, E., and Moormann, R. J. (1994) *Virology* **200,** 558–565
15. Bruschke, C. J., Moormann, R. J., van Oirschot, J. T., and van Rijn, P. A. (1997) *Vaccine* **15,** 1940–1945
16. Schwarze, S. R., Hruska, K. A., and Dowdy, S. F. (2000) *Trends Cell. Biol.* **10,** 290–295
17. Derossi, D., Chassaing, G., and Prochiantz, A. (1998) *Trends Cell. Biol.* **8,** 84–87
18. Lindgren, M., Hallbrink, M., Prochiantz, A., and Langel, U. (2000) *Trends Pharmacol. Sci.* **21,** 99–103
19. Ruggli, N., Moser, C., Mitchell, D., Hofmann, M., and Tratschin, J. D. (1995) *Virus Genes* **10,** 115–126
20. Lamy, B., and Davies, J. (1991) *Nucleic Acids Res.* **19,** 1001–1006
21. Zasloff, M. (1987) *Proc. Natl. Acad. Sci. U. S. A.* **84,** 5449–5453
22. Fields, C. G., Lloyd, D. H., Macdonald, R. L., Otteson, K. M., and Noble, R. L. (1991) *Pept. Res.* **4,** 95–101
23. Matsuzaki, K., Sugishita, K., Fujii, N., and Miyajima, K. (1995) *Biochemistry* **34,** 3423–3429
24. Franklin, A. L., and Filion, W. G. (1981) *Stain Technol.* **56,** 343–348
25. Gasset, M., Mancheno, J. M., Lacadena, J., Turnay, J., Olmo, N., Lizarbe, M. A., Martinez del Pozo, A., Onaderra, M., and Gavilanes, J. G. (1994) *Curr. Top. Pept. Protein. Res.* **1,** 99–104
26. Schindler, D. G., and Davies, J. E. (1977) *Nucleic Acids Res.* **4,** 1097–1110
27. Yang, X., and Moffat, K. (1996) *Structure* **4,** 837–852
28. Mancheno, J. M., Gasset, M., Lacadena, J., Martinez del Pozo, A., Onaderra, M., and Gavilanes, J. G. (1995) *J. Theor. Biol.* **172,** 259–267
29. Matsuzaki, K. (1998) *Biochim. Biophys. Acta* **1376,** 391–400
30. Bellet-Amalric, E., Blaudez, D., Desbat, B., Graner, F., Gauthier, F., and Renault, A. (2000) *Biochim. Biophys. Acta* **1467,** 131–143
31. Mancheno, J. M., Gasset, M., Albar, J. P., Lacadena, J., Martinez del Pozo, A., Onaderra, M., and Gavilanes, J. G. (1995) *Biophys. J.* **68,** 2387–2395
32. Derossi, D., Calvet, S., Trembleau, A., Brunissen, A., Chassaing, G., and Prochiantz, A. (1996) *J. Biol. Chem.* **271,** 18188–18193
33. Pooga, M., Soomets, U., Hallbrink, M., Valkna, A., Saar, K., Rezaei, K., Kahl, U., Hao, J. X., Xu, X. J., Wiesenfeld-Hallin, Z., Hokfelt, T., Bartfai, T., and Langel, U. (1998) *Nat. Biotechnol.* **16,** 857–861
34. Vives, E., Brodin, P., and Lebleu, B. (1997) *J. Biol. Chem.* **272,** 16010–16017